Received: 5 June 2019 | Revised: 8 July 2019 | Accepted: 10 July 2019

DOI: 10.1002/jsp2.1061

RESEARCH ARTICLE

JOR Spine OPEN ACCESS

Slow depressurization following intradiscal injection leads to injectate leakage in a large animal model

Lara J. Varden[1] | Duc T. Nguyen[2] | Arthur J. Michalek[2]

[1]Interdisciplinary Bioscience and Biotechnology Program, Clarkson University, Potsdam, New York

[2]Department of Mechanical and Aeronautical Engineering, Clarkson University, Potsdam, New York

Correspondence
Arthur J. Michalek, Department of Mechanical and Aeronautical Engineering, Clarkson University, Box 5725, Potsdam, NY, 13699.
Email: ajmichal@clarkson.edu

Abstract

Needle injection has been indicated as the most practical method of delivering therapeutic agents to the intervertebral disc due to the disc's largely avascular nature. As the disc is characterized by both high stiffness and low permeability, injection requires substantial pressure, which may not relax on practical time scales. Additionally, needle puncture results in a localized disruption to the annulus fibrosus that can provide a leakage pathway for pressurized injectate. We hypothesized that intradiscal injection would result in slow relaxation of injectate pressure, followed by leakage upon needle retraction. This hypothesis was tested via controlled injection of fluorescently labeled saline into bovine caudal discs via a 21 gauge needle. Injections were performed with 10% of total disc volume injected at 3%/s followed by a 4-minute dwell. An analytical poroelastic model was calibrated to the experimental data and used to estimate injectate delivery with time. Experimental results confirmed both pressurization (with a peak of 199 ± 45 kPa) and slow recovery (final pressure of 81 ± 23 kPa). Injectate leakage through the needle puncture was verified following needle retraction in all samples. Histological sections of the discs displayed a clear defect at each disc's injection site with strong fluorescent labeling indicating a leakage pathway. The modeling results suggest that less than one-fourth of the injected volume was absorbed by the tissue in 4 minutes. Taken together these results suggest that needle injection is a feasible, albeit inefficient method for delivery of therapeutic agents into the intervertebral disc. Particular care should be taken to aspirate un-absorbed injectate prior to needle retraction to prevent leakage and exposure of surrounding tissues.

KEYWORDS

5-DTAF, bovine caudal, intervertebral disc, needle puncture, poroelastic model

1 | INTRODUCTION

The intervertebral disc (IVD) is a fibrocartilaginous structure consisting of a highly hydrated inner nucleus pulposus (NP) surrounded by a ligamentous annulus fibrosus (AF) providing flexible connectivity between vertebral bones. Degeneration of the IVD is a contributor to low back pain, which is the most prevalent cause of disability worldwide[1] having an economic burden on the United States of around $100 billion a year.[2,3] Development of safe and effective treatments for disc degeneration is critical for the reduction of this public health burden.[4,5]

As the IVD is nearly avascular, needle injection is the most practical mode of delivery for therapeutic agents including stem cells,[6]

growth factors,[7] siRNA,[8] synthetic extracellular matrix proteins,[9] and structural modifiers.[10] Retention of injectate within the disc is critical for both efficacy of treatment and minimization of harmful side effects. Post-injection leakage has been identified as a potential limitation of cell-based therapies for disc degeneration.[6] While substantial loss of cells following injection has been observed,[11] other injectates are often untraced in experiments. Side effects potentially attributed to injectate leakage range from osteophyte formation[12] to paralysis.[13] There are currently no widely adopted standards for the development of intradiscal injection protocols, particularly with the aim of reducing post-injection leakage.

During needle injection, fluid enters the tissue at a single point. In high permeability tissues, relatively low injection pressure results in rapid percolation of injectate. In low permeability tissues, fluid is injected more rapidly than it may percolate resulting in deformation of the tissue. The fluid pressure required for this deformation depends on the stiffness of the tissue. As the IVD consists of a relatively low permeability NP constrained by a stiff AF, this process results in large pressures during injection.[14] Additionally, low permeability of the NP is implicated in slow relaxation of induced fluid pressure.[15,16] It is currently unknown quantitatively how stiffness and permeability affect both pressurization and relaxation rates during intradiscal injection.

Needle puncture of the AF is known to result in localized tissue disruption of the tissue with both mechanical[17–19] and biological[20,21] consequences. In small animal IVDs, proportional decrease with stiffness with increasing puncture size[22] is consistent with fluid flow through the needle track.[23] It is thus likely that unabsorbed injectate, if still under pressure due to slow relaxation, may be forced out through the track following needle retraction, resulting in leakage.

Taken together, prior research on intradiscal injection has indicated pressurization during injection, slow relaxation, a pathway for injectate leakage, and adverse effects on adjacent tissues. The mechanisms through which these phenomena might be related remain unknown. We hypothesized that the high stiffness and low permeability of the IVD would result in pressurization during intradiscal injection followed by slow relaxation. Furthermore, residual pressure following injection was hypothesized to result in injectate leakage through the needle track following needle retraction. This hypothesis was tested by performing controlled injections into bovine caudal intervertebral discs. Injectate delivery and leakage was assessed using a fluorescent dye. An analytical poroelastic model of pressurization during intradiscal injection was fit to the experimental data and used to estimate the amount of injectate delivered with time.

2 | METHODS

2.1 | Experiment

Controlled fluid injection into fresh bovine caudal IVDs was used to measure pressurization and relaxation. Ten intervertebral discs were harvested within 24 hours of sacrifice from two skeletally mature bovine tails obtained from a local abattoir. The discs were separated from their adjacent vertebrae with a scalpel, and care was taken to maintain approximately constant height across the disc. During dissection, the anterior aspect of the AF was marked, and three measurements each of disc height and diameter were recorded. One disc was excluded from the study due to visual signs of pathology, namely drastically reduced disc height, vascular intrusion, and discoloration of the NP tissue.

The injector (Figure 1) consisted of a linear actuator connected to a 1 mL syringe and 21 gauge hypodermic needle (BD PrecisionGlide, Franklin Lakes, New Jersey). Between the syringe and needle, a series of high pressure pipe fittings were used to attach a fluid reservoir with valve (valve 1), a pressure transducer with panel meter (Omega Engineering, Norwalk, Connecticut), and a shutoff valve (valve 2). Both the linear actuator and pressure transducer were connected to a computer via a data acquisition board (National Instruments, Austin, Texas). The injector was filled with 0.135 M phosphate-buffered saline (pH 7.4) along with 0.05 mg/mL 5-DTAF (Sigma-Aldrich, St. Louis, Missouri). The addition of fluorescent (492 nm absorption and 516 nm emission) 5-DTAF was used to both visualize injectate delivery into the tissue and indicate leakage in the injector fittings. Complete purging of air bubbles from the system was confirmed by manually pressing the syringe plunger while both valves were closed and confirming less than 10 μL displacement at 1 MPa measured pressure.

Excised IVDs were placed between a pair of sintered stainless steel platens (1.5″ diameter, 1/16″ thickness, and 40 μm pore size, Applied Porous Technologies, Tariffville, Connecticut) attached to flat nylon plates. The nylon plates were connected by a pair of threaded posts with wing nuts, which were used to adjust their spacing to constrain the disc axially without an initial compressive preload. The injector needle was then inserted radially into the posterolateral aspect of the disc to a depth of one half of the disc diameter. After placement of the needle into the IVD, valve 2 was opened and valve 1 was closed. During dissection both height and diameter of each disc were measured and recorded. These were used to calculate total disc volumes. Disc volumes were used to program the linear actuator for each specimen to perform a ramp at constant rate, corresponding to 3%/s,

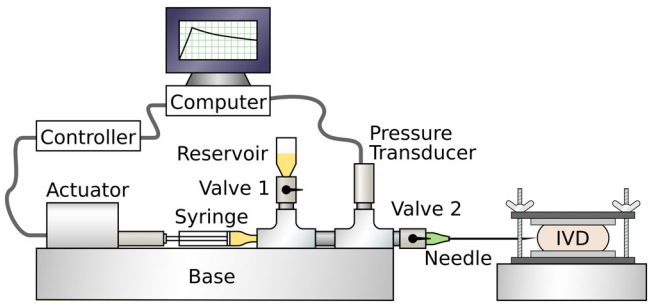

FIGURE 1 Schematic of experimental system. A linear actuator and syringe were used to perform injections with controlled volumes and rates while system pressure was recorded by the transducer. Valve 1 and reservoir were used to fill the system with fluorescently labeled saline. Valve 2 was used to prevent fluid flow into or out of the needle during retraction

to a final displacement corresponding to 10% of disc volume. The injection rate was determined during instrument testing to result in less than 1 kPa of back pressure. Following the ramp, displacement was held for 240 seconds, which was determined by a pilot study to be the minimum time required for an accurate model fit. Fluid pressure in the injector was sampled at 20 Hz throughout the test. At the end of the test, valve 2 was closed, and the disc was removed from the injector and frozen at −20°C.

Injectate delivery and leakage was assessed by taking 30 μm cryosections of the frozen discs at mid-height. The sections were mounted on plain glass slides (VWR, Radnor, Pennsylvania), air dried, and covered with coverslipping medium (Polysciences, Warrington, Pennsylvania). Slides were imaged using an inverted microscope (Olympus, Waltham, Massachusetts) equipped with a 2.5× objective and digital camera. Epifluorescence with a fluorescein filter set was used to visualize 5-DTAF staining, and crossed polarizing filters were used to image AF tissue structure. Additionally, photographs were taken of each disc after sectioning using a stereomicroscope (AmScope Inc., Irvine, California) equipped with a green lens filter and 24 W LED lamp with 450 to 460 nm emission (ABI, Indianapolis, Indiana).

2.2 | Model

A nonlinear poroelastic model was used to describe the experimental pressure vs volume behavior. Injection site pressure was modeled analytically with injection volume, *V(t)* normalized to disc volume. The model considered the point of injection (Figure 2) with inflow from the needle, outflow into the surrounding tissue, and nonlinear elastic storage. The volumetric flow rate into and out of the injection site was accounted for by input rate, Q_I (s^{-1}), and porous outflow into surrounding tissue, with effective permeability, k (Pas^{-1}), driven by the gradient between internal pressure, *p(t)* (Pa) and atmospheric pressure outside of the disc. It is assumed that fluid flows radially outwards through the tissue away from the injection site. The effective permeability term describes the average resistance to flow across all directions and distances from the injection site.

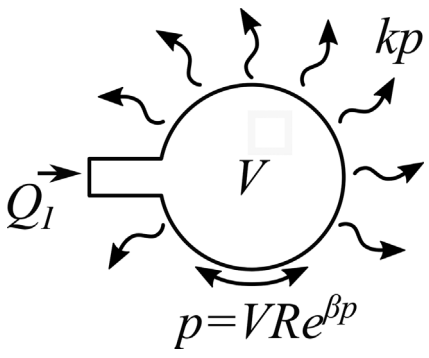

FIGURE 2 Schematic representation of the control volume analyzed by the analytical model. Fluid may move into the volume through injection (with rate, Q_I) and out through porous flow with effective permeability, k. Transient storage is accounted for by nonlinear compliance (with linear term, R, and nonlinear term, β) of the tissue

$$\frac{dV(t)}{dt} = Q_I - kp(t) \tag{1}$$

The pressure-volume relationship at the injection site was described by a function determined empirically during pilot testing to produce an accurate fit to experimental data. Intradiscal fluid pressure increased nonlinearly with fluid volume, defined by stiffness, R (Pa), and exponent, β (Pa^{-1}). Stiffness, R, describes a linear increase in pressure with injection volume, while exponent, β, describes stiffening of the tissue at higher pressure. It is assumed in this model that both injection and relaxation rates are slow enough to be insensitive to viscoelastic effects.

$$p(t) = V(t)Re^{\beta p(t)} \tag{2}$$

Combining Equations (1) and (2) and solving for rate of pressure change yields the following governing equation.

$$\frac{dp(t)}{dt} = \frac{(Q_I - kp(t))Re^{\beta p(t)}}{1 - \beta p(t)} \tag{3}$$

For a typical ramp-hold injection protocol, input rate, Q_I, was defined as constant during injection and zero during relaxation. The governing equation was solved for *p(t)* via MATLAB (Mathworks Inc., Natick, Massachusetts) using a fourth-order Runge-Kutta routine with an initial pressure of zero and a time step of 0.05 seconds.

The analytical model was fit to each experimental pressure vs time trace. Given experimental Q_I, a simplex algorithm (fminsearch in MATLAB) was used to vary model parameters, k, R, and β, in order to minimize the error between predicted and experimental pressure. The best-fit pressure vs time trace was stored for each test. Additionally, pressure and best fit effective permeability were used to calculate the volume of injectate which exited the injection site into the surrounding tissue in total time, τ. This represents the total volume of injectate (normalized to disc volume) delivered to the disc with time.

$$V_{\text{Delivered}}(\tau) = \int_0^{\tau} kp(t)dt \tag{4}$$

3 | RESULTS

All discs exhibited pressurization during injection, with a peak pressure of 199 ± 45 kPa. At the end of the 4-minute dwell, pressure relaxed to an average of 81 ± 23 kPa. Injectate leakage was visually observed on the outside surfaces of all discs following needle retraction. Photographs of the discs (Figure 3A) showed diffuse labeling in the NP, along with clear labeling around the needle track and along the posterolateral outer AF surface. Fluorescent micrographs

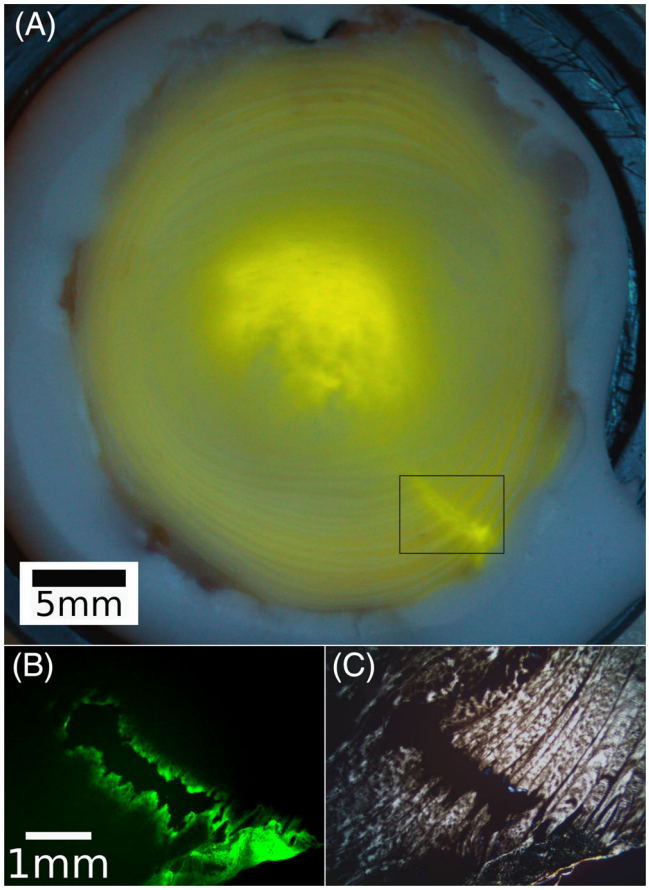

FIGURE 3 A, Photograph of injected disc, transected at mid-height, showing 5-DTAF delivery to the nucleus pulposus (NP) as well as the track to the point of injection. The diffuse signal in the annulus fibrosus (AF) has been confirmed in un-injected control specimens to be the result of collagen autofluorescence. B, Fluorescent micrograph of the boxed area in A, showing 5-DTAF binding to the walls of the needle track. C, Polarized light micrograph of same area, showing a clear disruption of the AF structure

(Figure 3B) showed large amounts of 5-DTAF in the needle tracks and on the outside surfaces of the discs. Polarized light micrographs (Figure 3C) showed disruption to the AF structure at the needle track, comparable in width to the 0.82 mm diameter of the needle.

Experimentally measured pressure vs time signals were well fit by the analytical model (Figure 4), with average parameter values of $R = 727 \times 10^{-3} \pm 275 \times 10^{-3}$ Pa, $\beta = 5.8 \times 10^{-6} \pm 2.1 \times 10^{-6}$ Pa^{-1}, and $k = 950 \times 10^{-12} \pm 287 \times 10^{-12}$ $(Pas)^{-1}$. The model fits (Figure 5A) produced a slight underestimate (174 ± 57 kPa) of experimental peak pressure, but a consistent estimate (81 ± 25 kPa) of final residual pressure. Based on the rate of pressure relaxation and best-fit values of k, the model estimated an average delivered injectate volume (Figure 5B) of 2.375 ± 0.569% of total disc volume at the end of 240 seconds.

4 | DISCUSSION

The present study confirms earlier observations of intradiscal pressurization during the injection.[14,15,24] Peak pressures (~200 kPa)

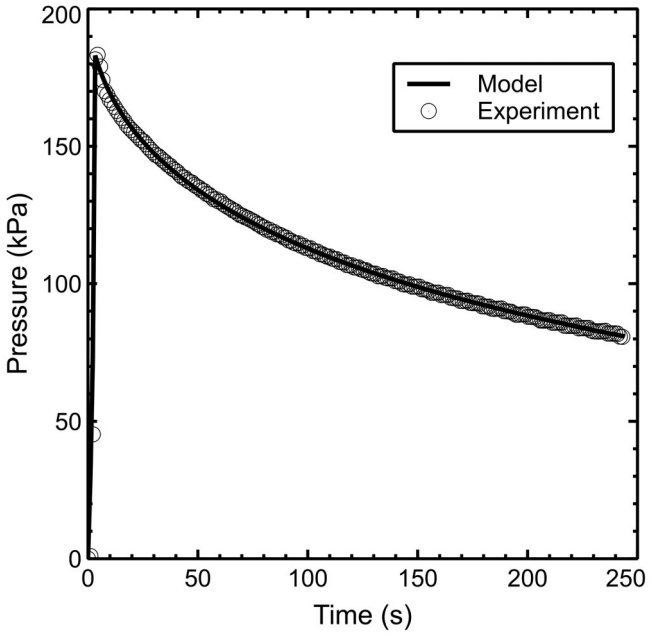

FIGURE 4 Analytical model fit to typical experimental pressure vs time data. Experimental data has been downsampled for clarity

were comparable to those used in provocative discography,[25] and were well below the rupture pressures (1-5 MPa) reported by Wang et al for both human and porcine IVDs injected through a 21 g needle.[14] Signs of rupture, such as a non-monotonic increase in pressure during the injection phase of the experiment, were not observed in our study. The fluorescent dye observed in the needle tracks (Figure 3) is thus most likely to have been deposited following needle retraction.

Experimental pressurization and relaxation were well fit by an analytical model representing fluid flow into and out of the injection site, with storage of excess fluid accounted for by nonlinear deformation of the surrounding tissue. Our fit parameters suggest that the response is highly nonlinear at experimental pressure magnitude. This is consistent with pressure vs volume response in human lumbar IVDs,[24] which showed little pressurization at small volumes. Model predictions of volume delivered (Figure 5B) were in qualitative agreement with fluorescent dye experiments (Figure 3A), suggesting that approximately one-quarter of the injected fluid was absorbed by the tissue prior to needle retraction. An important avenue of future research is determination of threshold residual pressure below which leakage will not occur.

While the experimental injections were performed with a linear actuator for the purpose of repeatability, they were generally representative of manual injection. The peak pressures measured in this study correspond to a force of approximately 4 to 5 N applied to a 1 mL syringe, which is less than one-tenth of the average maximum thumb force reported in the literature.[26] The fluorescent dye measurements (Figure 3) likely overestimate the amount of injectate delivered in a typical clinical or laboratory protocol, as a post-injection dwell of 4 minutes is impractical in those settings.

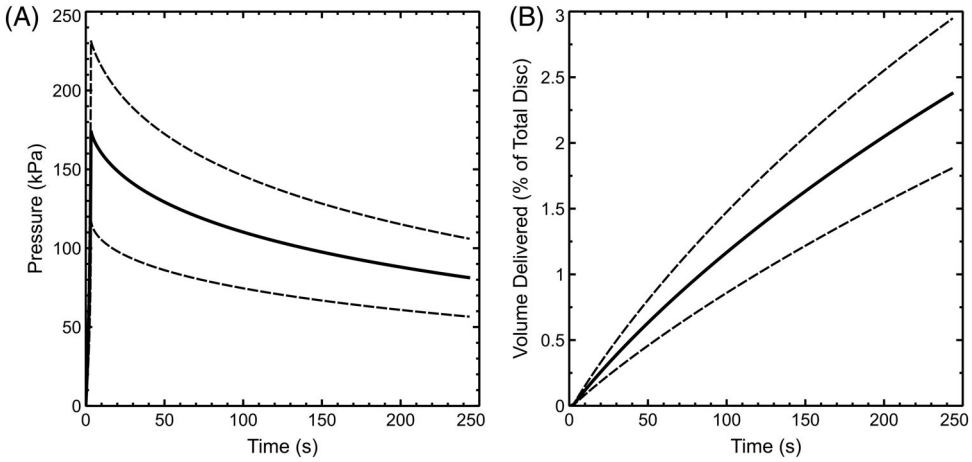

FIGURE 5 Average ± SD model predictions of pressure (A) and delivered volume of injectate (B) during experimental injection of 10% total disc volume

Our experiments were performed with excised discs constrained by porous metal platens, a common boundary condition in organ culture systems.[27–29] This condition was chosen for the present study to allow freezing and cryosectioning of the discs with minimal handling after injection, which was presumed to affect dye distribution. Pilot studies found no differences in either peak pressure or rate of depressurization between excised discs and discs still attached to adjacent vertebrae. This suggests that pressurization is dictated by radial bulging, and relaxation is limited by the permeability of the NP and AF rather than the vertebral endplates.

The present study was performed using bovine caudal IVDs due to their availability, low interspecimen variability, and common use as a pre-clinical model. Despite differences in size and shape, bovine caudal discs are compositionally and mechanically similar to healthy human lumbar discs at the tissue level.[30] When scaled by an approximate human lumbar disc volume of 16 mL,[31] previously reported[24] injection stiffness range from 22 kPa/% to 87 kPa/%. The bovine caudal values were comparable, with an average of 20 kPa/%, and a peak of over 50 kPa/% at maximum injection volume. Although the bovine discs used in this study were young and free of pathology, AF tissue stiffness remains relatively constant with degeneration.[32,33] In human lumbar discs, this results in relatively constant peak pressure during injection.[15] Human lumbar discs have been shown to depressurize more rapidly with degeneration,[15] however, the residual pressure after 2 minutes in all but the most severe degenerative grades (~60 kPa) was above the residual pressure at which we observed leakage in the present study. It is possible that faster relaxation in degenerated discs is the result of flow through radial fissures,[34] which may provide additional pathways for leakage of injectate outside of the disc.

This study utilized a combination of experimental and modeling techniques to address the question of whether or not intradiscal injection procedures can be performed without post-injection leakage. The combination of high stiffness and low permeability in the IVD results in injectate pressurization that does not relax on clinically practical time scales. Substantial damage to the AF by the needle puncture gives the pressurized injectate a ready pathway for leakage following needle retraction. Our findings suggest that while needle injection may be used for successful delivery into the IVD, efficiency of delivery is low, and aspiration of un-absorbed injectate prior to needle retraction may be necessary to minimize leakage risk.

ACKNOWLEDGMENTS

The authors thank Christopher Nicolella for assistance with instrumentation development and Ward Willard & Son of Heuvelton, NY for specimens.

CONFLICT OF INTEREST

The authors have no conflicts, financial or otherwise, related to this work.

AUTHOR CONTRIBUTIONS

L.J.V., D.T.N., and A.J.M. designed the experimental study and performed measurements. D.T.N and A.J.M. developed the analytical model. All authors reviewed and approved the manuscript.

ORCID

Arthur J. Michalek https://orcid.org/0000-0001-9417-9344

REFERENCES

1. Hartvigsen J, Hancock MJ, Kongsted A, et al. What low back pain is and why we need to pay attention. *Lancet*. 2018;*391*(10137):2356-2367.
2. Crow WT, Willis DR. Estimating cost of care for patients with acute low back pain: a retrospective review of patient records. *J Am Osteopath Assoc*. 2009;*109*(4):229-233.
3. Ma VY, Chan L, Carruthers KJ. Incidence, prevalence, costs, and impact on disability of common conditions requiring rehabilitation in the United States: stroke, spinal cord injury, traumatic brain injury, multiple sclerosis, osteoarthritis, rheumatoid arthritis, limb loss, and back pain. *Arch Phys Med Rehabil*. 2014;*95*(5):986-995 e981.
4. Buchbinder R, van Tulder M, Oberg B, et al. Low back pain: a call for action. *Lancet*. 2018;*391*(10137):2384-2388.

5. Foster NE, Anema JR, Cherkin D, et al. Prevention and treatment of low back pain: evidence, challenges, and promising directions. *Lancet*. 2018;*391*(10137):2368-2383.
6. Smith LJ, Silverman L, Sakai D, et al. Advancing cell therapies for intervertebral disc regeneration from the lab to the clinic: recommendations of the ORS spine section. *JOR Spine*. 2018;*1*(4):e1036.
7. Matta A, Karim MZ, Gerami H, et al. NTG-101: a novel molecular therapy that halts the progression of degenerative disc disease. *Sci Rep*. 2018;*8*(1):16809.
8. Banala RR, Vemuri SK, Dar GH, et al. Efficiency of dual siRNA-mediated gene therapy for intervertebral disc degeneration (IVDD). *Spine J*. 2019;*19*(5):896-904.
9. Prudnikova K, Lightfoot Vidal SE, Sarkar S, et al. Aggrecan-like biomimetic proteoglycans (BPGs) composed of natural chondroitin sulfate bristles grafted onto a poly(acrylic acid) core for molecular engineering of the extracellular matrix. *Acta Biomater*. 2018;*75*:93-104.
10. Lin HJ, Lin LC, Hedman TP, Chen WP, Chuang SY. Exogenous crosslinking restores Intradiscal pressure of injured porcine intervertebral discs: an in vivo examination using quantitative Discomanometry. *Spine (Phila Pa 1976)*. 2015;*40*(20):1572-1577.
11. Bertram H, Kroeber M, Wang H, et al. Matrix-assisted cell transfer for intervertebral disc cell therapy. *Biochem Biophys Res Commun*. 2005;*331*(4):1185-1192.
12. Vadala G, Sowa G, Hubert M, Gilbertson LG, Denaro V, Kang JD. Mesenchymal stem cells injection in degenerated intervertebral disc: cell leakage may induce osteophyte formation. *J Tissue Eng Regen Med*. 2012;*6*(5):348-355.
13. Wallach CJ, Kim JS, Sobajima S, et al. Safety assessment of intradiscal gene transfer: a pilot study. *Spine J*. 2006;*6*(2):107-112.
14. Wang JL, Tsai YC, Wang YH. The leakage pathway and effect of needle gauge on degree of disc injury post anular puncture: a comparative study using aged human and adolescent porcine discs. *Spine (Phila Pa 1976)*. 2007;*32*(17):1809-1815.
15. Brock M, Lutze M. Lumbar disk compliance and degeneration. *Surg Neurol*. 1989;*32*(1):11-15.
16. Michalek AJ, Iatridis JC. Height and torsional stiffness are most sensitive to annular injury in large animal intervertebral discs. *Spine J*. 2012;*12*(5):425-432.
17. Elliott DM, Yerramalli CS, Beckstein JC, Boxberger JI, Johannessen W, Vresilovic EJ. The effect of relative needle diameter in puncture and sham injection animal models of degeneration. *Spine (Phila Pa 1976)*. 2008;*33*(6):588-596.
18. Michalek AJ, Buckley MR, Bonassar LJ, Cohen I, Iatridis JC. The effects of needle puncture injury on microscale shear strain in the intervertebral disc annulus fibrosus. *Spine J*. 2010a;*10*(12):1098-1105.
19. Vergari C, Mansfield JC, Chan D, Clarke A, Meakin JR, Winlove PC. The effects of needle damage on annulus fibrosus micromechanics. *Acta Biomater*. 2017b;*63*:274-282.
20. Carragee EJ, Don AS, Hurwitz EL, Cuellar JM, Carrino JA, Herzog R. 2009 ISSLS prize winner: does discography cause accelerated progression of degeneration changes in the lumbar disc: a ten-year matched cohort study. *Spine (Phila Pa 1976)*. 2009;*34*(21):2338-2345.
21. Korecki CL, Costi JJ, Iatridis JC. Needle puncture injury affects intervertebral disc mechanics and biology in an organ culture model. *Spine (Phila Pa 1976)*. 2008;*33*(3):235-241.
22. Michalek AJ, Funabashi KL, Iatridis JC. Needle puncture injury of the rat intervertebral disc affects torsional and compressive biomechanics differently. *Eur Spine J*. 2010b;*19*(12):2110-2116.
23. Michalek AJ, Iatridis JC. Penetrating annulus fibrosus injuries affect dynamic compressive behaviors of the intervertebral disc via altered fluid flow: an analytical interpretation. *J Biomech Eng*. 2011;*133*(8):084502.
24. Ranu HS. Multipoint determination of pressure-volume curves in human intervertebral discs. *Ann Rheum Dis*. 1993;*52*(2):142-146.
25. Derby R, Lee SH, Lee JE, Lee SH. Comparison of pressure-controlled provocation discography using automated versus manual syringe pump manometry in patients with chronic low back pain. *Pain Med*. 2011;*12*(1):18-26.
26. MacDonald V, Wilson K, Sonne MWL, Keir PJ. Grip type alters maximal pinch forces in syringe use. *Hum Factors*. 2017;*59*(7):1088-1095.
27. Chan SC, Walser J, Ferguson SJ, Gantenbein B. Duration-dependent influence of dynamic torsion on the intervertebral disc: an intact disc organ culture study. *Eur Spine J*. 2015;*24*(11):2402-2410.
28. Jim B, Steffen T, Moir J, Roughley P, Haglund L. Development of an intact intervertebral disc organ culture system in which degeneration can be induced as a prelude to studying repair potential. *Eur Spine J*. 2011;*20*(8):1244-1254.
29. Korecki CL, MacLean JJ, Iatridis JC. Characterization of an in vitro intervertebral disc organ culture system. *Eur Spine J*. 2007;*16*(7):1029-1037.
30. Demers CN, Antoniou J, Mwale F. Value and limitations of using the bovine tail as a model for the human lumbar spine. *Spine (Phila pa 1976)*. 2004;*29*(24):2793-2799.
31. Zhou SH, McCarthy ID, McGregor AH, Coombs RR, Hughes SP. Geometrical dimensions of the lower lumbar vertebrae--analysis of data from digitised CT images. *Eur Spine J*. 2000;*9*(3):242-248.
32. O'Connell GD, Sen S, Elliott DM. Human annulus fibrosus material properties from biaxial testing and constitutive modeling are altered with degeneration. *Biomech Model Mechanobiol*. 2012;*11*(3–4):493-503.
33. Vergari C, Chan D, Clarke A, Mansfield JC, Meakin JR, Winlove PC. Bovine and degenerated human annulus fibrosus: a microstructural and micromechanical comparison. *Biomech Model Mechanobiol*. 2017a;*16*(4):1475-1484.
34. Adams MA, Hutton WC. The mechanics of prolapsed intervertebral disc. *Int Orthop*. 1982;*6*(4):249-253.

How to cite this article: Varden LJ, Nguyen DT, Michalek AJ. Slow depressurization following intradiscal injection leads to injectate leakage in a large animal model. *JOR Spine*. 2019;2:e1061. https://doi.org/10.1002/jsp2.1061